

See discussions, stats, and author profiles for this publication at: <https://www.researchgate.net/publication/26826777>

Alkylamino Hydrazide Derivatives of Hyaluronic Acid: Synthesis, Characterization in Semidilute Aqueous Solutions, and Assembly into Thin Multilayer Films

ARTICLE *in* BIOMACROMOLECULES · SEPTEMBER 2009

Impact Factor: 5.75 · DOI: 10.1021/bm900701m · Source: PubMed

CITATIONS

10

READS

48

8 AUTHORS, INCLUDING:



Di Cui

Institut Curie - Hôpital René Huguenin

7 PUBLICATIONS 150 CITATIONS

[SEE PROFILE](#)



Claire Nicolas

French Institute of Health and Medical Res...

11 PUBLICATIONS 307 CITATIONS

[SEE PROFILE](#)



Karine Glinel

Université catholique de Louvain

55 PUBLICATIONS 1,805 CITATIONS

[SEE PROFILE](#)



Catherine Picart

Ecole de Physique, Electronique et Matéria...

147 PUBLICATIONS 7,406 CITATIONS

[SEE PROFILE](#)

Alkylamino Hydrazide Derivatives of Hyaluronic Acid: Synthesis, Characterization in Semidilute Aqueous Solutions, and Assembly into Thin Multilayer Films

Shirin Kadi,[†] Di Cui,[†] Eric Bayma,[†] Thomas Boudou,[‡] Claire Nicolas,[‡] Karine Glinel,[§] Catherine Picart,^{*,‡} and Rachel Auzély-Velty^{*,†}

Centre de Recherches sur les Macromolécules Végétales (CERMAV-CNRS), BP53, F-38041 Grenoble cedex 9, France, Minatec, Grenoble Institute of Technology and LMGP, 3 parvis Louis Néel, F-38016 Grenoble Cedex, France, and Laboratoire Polymères, Biopolymères, Surfaces, Université de Rouen - CNRS, Bd Maurice de Broglie, F-76821 Mont-Saint-Aignan, France

Received June 20, 2009; Revised Manuscript Received September 1, 2009

A series of biodegradable alkylamino hydrazide hyaluronic acid (HA) derivatives were prepared and used to design new biocompatible films able to release hydrophobic drugs in a controlled manner. The first step of this work thus consisted in optimizing the synthetic conditions of hydrazide HA derivatives bearing pendant hexyl, octyl, decyl, and citronellyl chains with a degree of substitution of 0.05 or 0.10. The behavior in aqueous solution of these water-soluble modified HA samples was then examined in the semidilute regime. The decylamino hydrazide derivatives of HA exhibited remarkable associating properties, giving rise to transparent gels. These gels were found to be more resistant to degradation by hyaluronidase compared to solutions of nonmodified HA at the same concentration. The other derivatives of which the lengths of grafted alkyl chains range from 6 to 8 carbon atoms lead to more or less viscous solutions. Different viscometric features for these derivatives could be observed as a function of the molecular weight of HA. As derivatives prepared from a HA sample of 600 000 g/mol (HA-600) exhibited a much higher tendency to self-aggregate than their counterparts prepared from a HA sample of 200 000 g/mol (HA-200), the latter derivatives were selected for the build up of multilayer films. The topography and z-section of (PLL/HA derivatives) films assembled layer-by-layer were observed by atomic force microscopy (AFM) in liquid and confocal laser scanning microscopy (CLSM) using PLL^{FITC} as ending layer. Moreover, the ability of the films made of the different HA derivatives to incorporate the hydrophobic dye nile red (NR) was investigated. Films containing decylamino hydrazide HA derivatives were the most efficient for incorporating and retaining nile red, which confirms the formation of stable hydrophobic nanodomains in the films.

Introduction

In recent years, much attention has been focused on the development of biomaterials based on hyaluronic acid (HA), especially in the fields of tissue engineering, drug delivery, and viscosupplementation,^{1–8} owing to its unique physicochemical properties and biological functions. HA is a glycosaminoglycan found ubiquitously in the extracellular matrix of mammalian connective tissues.⁹ Previously, this linear polyanionic polymer, composed of repeating disaccharide units of *N*-acetyl-D-glucosamine and D-glucuronic acid, was believed to act only as an inert lubricating substance in tissues; however, important biological roles of HA are now widely reported in the literature.¹⁰ HA controls important functions regulating cellular proliferation and differentiation. Cellular interactions with HA occur through cell surface receptors (CD44, RHAMM, and ICAM-1) and influence processes such as morphogenesis, wound repair, and metastasis.^{11–13} HACD44 receptors are overexpressed in the tumor cell surface and they play a role in tumor cell migration.¹⁰ Due to these specific recognition properties,

HA has thus been proposed as a macromolecular carrier for antitumoral drugs. Other HA drug delivery systems based on hydrogels and microspheres have also been reported.^{6–8}

In a previous work, taking into account the biological and physicochemical properties of HA, we synthesized new alkylamino hydrazide derivatives of HA for the purpose to obtain thickeners or gelling polymers having potential applications in viscosupplementation, controlled drug delivery, and encapsulation of fragile materials.¹⁴ These HA derivatives being still water-soluble were shown to exhibit remarkable associating properties in the presence of external salt. Formation of hydrophobic domains was demonstrated from fluorescence measurements in the presence of pyrene as a probe. Transparent hydrogels were especially obtained for derivatives having decyl chains.

Following recent results showing the ability to prepare multilayers made of hydrophobically modified poly(ethylene oxide)^{15,16} and the ability of hydrophobically modified carboxymethyl pullulan (CMP) derivatives and poly(ethylenimine) to entrap hydrophobic dye molecules in hydrophobic nanoreservoirs made of the pendant alkyl chains grafted on CMP,¹⁷ we investigated the possibility to exploit the amphiphilic nature of our alkylamino hydrazide HA derivatives to produce versatile delivery platforms for hydrophobic drugs. To date, very few examples of planar multilayer films based on HA playing the role of reservoirs for hydrophobic drugs have been reported. The hydrophobic antitumor drug Paclitaxel was loaded by

* To whom correspondence should be addressed. E-mail: rachel.auzely@cermav.cnrs.fr (R.A.-V.); catherine.picart@minatec.grenoble-inp.fr (C.P.). Phone: +33(0)476037671 (R.A.-V.); +33(0)4 56 52 93 11 (C.P.). Fax: +33(0)476547203 (R.A.-V.); +33(0)476 56 52 93 01 (C.P.).

[†] CERMAV-CNRS, affiliated with Université Joseph Fourier, and member of the Institut de Chimie Moléculaire de Grenoble.

[‡] Minatec, Grenoble Institute of Technology and LMGP.

[§] Université de Rouen - CNRS.

simple postdiffusion in cross-linked polyelectrolyte multilayer films made of poly(L-lysine)/hyaluronic acid (PLL/HA)₁₂ films¹⁸ (i.e., made of 12 layer pairs) or in (PLL/HA)₃₀ films capped by (PSS/PAH) layers.¹⁹ In this latter case, PSS/PAH layers were added to render adhesive the initially non adhesive (PLL/HA)₃₀ film. These films, which are characterized by an exponential growth of their thickness with the number of deposited layer pairs, can potentially play the role of a reservoir for the drug. However, the amount of hydrophobic drug loaded in (PLL/HA) films is limited by the affinity of the drug with the film components, which are hydrophilic. Another approach consisted in introducing a labile ester linkage between paclitaxel and HA (called prodrug approach) to prepare multilayer based on chitosan and HA-paclitaxel.²⁰ However, this strategy is limited to hydrophobic drugs possessing a functionality allowing their controlled chemical grafting on the polymer chain. In the present study, we synthesized a new series of alkylamino hydrazide HA derivatives by varying the degree of substitution (DS), the nature of the alkyl chain, and the molecular weight of HA to produce films with tunable entrapment and release properties. We first optimized the synthetic conditions as described in the first section of the present paper. Then, we investigated the behavior of the amphiphilic derivatives in the bulk and their enzymatic degradability by rheological measurements. Finally, we explored the possibility to deposit the alkylamino hydrazide derivatives as thin multilayer films in combination with PLL as polycation as well as their ability to trap and retain a hydrophobic dye, nile red.

Experimental Section

Materials. The sample of bacterial sodium hyaluronate with a molar mass of 6×10^5 g/mol (HA-600) was supplied by ARD (Pomacle, France) and that with a molar mass of 2×10^5 g/mol (HA-200) was purchased from MEDIPOL Distribution. The molar mass distribution and the weight-average molar mass of HAs were determined by size exclusion chromatography using a Waters GPCV Alliance 2000 chromatograph (U.S.A.) equipped with three online detectors: a differential refractometer, a viscometer, and a light scattering detector (MALLS) from Wyatt (U.S.A.); the solutions were injected at a concentration of 5×10^{-4} g/mL in 0.1 M NaNO₃. The polydispersity of the samples, referred to as HA-200 and HA-600, is $M_w/M_n \sim 1.5$. The overlap concentration C^* of HA-200 and HA-600 in 0.01 M phosphate buffered saline (PBS, pH 7.4) solution containing 0.154 M NaCl at 25 °C is around 2.4 and 0.9 g/L, respectively. These values were derived from the intrinsic viscosity, assuming that $C^*[\eta]$ is about unity.²¹ The aldehydic chains, 1-hexanal, 1-octanal, 1-decanal, and (\pm)-citronellal, the hydrophobic dye nile red (NR; ref 19123), and all other chemicals were purchased from Sigma-Aldrich-Fluka. The water used in all experiments was purified by a Millipore Milli-Q Plus purification system, with a resistivity of 18.2 MΩ cm.

NMR Spectroscopy. ¹H NMR spectra of the alkylamino hydrazide derivatives dissolved in deuterium oxide (6 mg/mL) were performed at 80 °C using a Bruker DRX400 spectrometer operating at 400 MHz. Deuterium oxide was obtained from SDS (Vitry, France).

Dilute Solution Viscometry. The intrinsic viscosities were determined by measuring viscosity of polymer solutions at low concentrations (<1 g/L) with an Ubbelohde capillary viscometer ($\phi = 0.58$ mm) and extrapolating to infinite dilution using the Huggins equation²² as described below:

$$\eta_{sp}/C = [\eta] + k'[\eta]^2 C \quad (1)$$

In this relation, η_{sp} is the specific viscosity, C is the polymer concentration (g/mL), and k' is the Huggins constant. The intrinsic

viscosity $[\eta]$ for HA-200 and HA-600 in 0.01 M PBS (0.154 M NaCl, pH 7.4) at 25 °C was found to be equal to 412 and 1085 mL/g, respectively.

Rheological Experiments. Dynamic experiments were performed with a cone plate rheometer (AR2000 from TA Instruments). The cones used have diameters of 4 and 6 cm and an angle of 3° 59' and 1°, respectively. All the dynamic rheological data were checked as a function of strain amplitude to ensure that the measurements were performed in the linear viscoelastic region. Experiments were carried out at 25 °C with a film of silicone oil to avoid solvent evaporation. Flow experiments were carried out with the AR2000 rheometer or with a Contraves LS30 Low-Shear rheometer, depending on the sample viscosity. The alkylamino hydrazide HA derivatives were first dissolved in pure water at a concentration of 11.11 g/L. After stirring for 4–6 h at room temperature, the samples were kept in the refrigerator for ~12 h and then diluted by addition of concentrated PBS to obtain final solutions at a concentration of 10 g/L in PBS (0.154 M NaCl, pH 7.4).

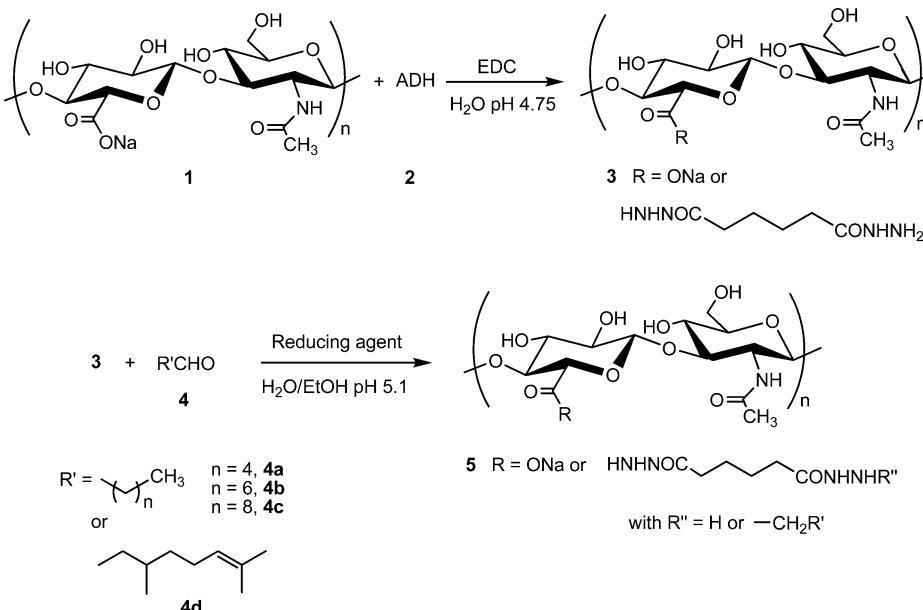
Studies of enzymatic degradation of solutions of HA modified with decyl chains and initial HA having a molecular weight M_w of 200000 or 600000 g/mol ($C_p = 10$ g/L) were performed using bovine testicular hyaluronidase (Hase from Sigma, type VIII, ~300 units/mg, ref H3757) at different concentrations in 0.01 M PBS (0.154 M NaCl, pH 7.4) at 37 °C. Kinetics of HA possessing decyl chains and initial HA depolymerization were measured with an AR2000 rheometer equipped with a Couette geometry (bob diameter 28 mm, height 42 mm, cup diameter 30 mm) or the cones described above, depending on the sample viscosity. The measurements started after equilibration for temperature at 37 °C, following addition of Hase (solubilized in a small volume of PBS) at room temperature. The time for equilibration temperature varied as a function of the geometry used: it was equal to 30 min in the case of the Couette geometry (sample volume = 8 mL) and 3 min when a cone was used (sample volume = 1.2 mL).

Synthesis. The alkylamino hydrazide derivatives of HA were synthesized according to the procedure described in Figure 1.

Hydrazide-Modified HA (HA-ADH 3) Derivatives. HA-ADH-600 (DS = 0.05) was prepared by dissolving HA-600 (4 g, 9.97 mmol) in pure water to a concentration of 1 g/L. Adipic dihydrazide (ADH; 1.73 g, 9.97 mmol) was added to this solution. The pH of the reaction was then adjusted to 4.75 using 0.5 M HCl. Next, an aqueous solution of 1-ethyl-3-[3-(dimethylamino)propyl] carbodiimide (EDC; 0.180 g, 0.935 mmol) was added slowly to the mixture. The pH of the reaction mixture was maintained at 4.75 by addition of 0.5 M HCl. The reaction was allowed to proceed at room temperature until no further change in pH was observed (i.e., 4 h). The reaction was stopped by addition of 0.05 M NaOH, raising the pH of reaction mixture to 7.5. The modified HA (3) was purified by diafiltration through an ultramembrane Amicon YM 100. The diafiltration was stopped when the filtrate conductivity was lower than 10 μS, and the HA-ADH derivative was recovered by freeze-drying. The chemical integrity and purity of the final product were checked by ¹H NMR. Digital integration of the NMR signals arising from the anomeric protons of HA and methylene protons of ADH group gave a substitution degree of 0.05 per disaccharide repeat unit.

The synthesis of the other HA-ADH samples with DS = 0.05 or 0.1 from HA-200 and HA-600 was performed using a similar procedure; the amount of EDC was two times increased to prepare derivatives having a DS of 0.1.

Decylamino Hydrazide Derivative of HA-600 (DS = 0.05). To a solution of HA-ADH-600, having a DS of 0.05 (1 g, 2.43 mmol) in water (250 mL), was added EtOH (150 mL). The pH of the solution was then adjusted to 5.1 by the dropwise addition of a 0.1 M aqueous HCl solution. The aldehydic chain (1-decanal; 0.050 g, 0.170 mmol) was then added, followed by a solution of 2-picoline borane complex (PicBH₃; 0.130 g, 1.21 mmol) in ethanol (5 mL). After stirring for 24 h at room temperature, the pH of the reaction was then adjusted to 7.5 with aqueous 0.1 M NaOH. After addition of NaCl at a concentration of 0.5 M, the modified HA was precipitated with EtOH in the

**Figure 1.** Synthesis of alkylamino hydrazide HA derivatives.**Table 1.** Reaction Conditions for the Synthesis of Alkylamino Hydrazide HA Derivatives and Intermediate HA-ADH

final polymer	polysaccharide substrate	EDC/HA ^a	alkyl chain/ HA-ADH ^b	DS ^c
HA-ADH 3	HA-200 or 600	0.095		0.05
HA-ADH 3	HA-200 or 600	0.19		0.10
HA5Cy ^d 5a-d	HA-ADH (DS = 0.05)		0.07	0.05
HA10Cy ^d 5a-d	HA-ADH (DS = 0.10)		0.15	0.10

^a Number of molar equivalents of EDC with respect to the repeating disaccharide unit of HA. ^b Number of molar equivalents of alkyl chain with respect to the repeating disaccharide unit of HA-ADH. ^c Determined from ¹H NMR, with an accuracy of 10%. ^d y refers to the number of carbon atoms of the alkyl chain or citronellyl chains, as specified in the Experimental Section.

proportion EtOH/H₂O 3/2 (v/v). The precipitate was successively washed with different mixtures of EtOH/H₂O (7/3, 7.5/2.5, 8/2, 9/1) and then was filtered to give a HA derivative, HA5C10-600, possessing C10 chains with a DS of 0.05, as determined by ¹H NMR integration.

The synthesis of the other alkylamino hydrazide HA samples with different alkyl chains and DS was performed using the same procedure; the amount of the aldehydic chain was adapted to the desired degree of substitution (see Table 1).

The different polymers obtained from the linear alkyl chains (**4a**, **4b**, and **4c**) are designated as HA_xCy-*M*, where *M* is the weight average molar mass of the parent HA, *x* reflects the degree of substitution (DS; *x* = 100 DS), and *y* is the number of carbon atoms of the grafted alkyl chain. The derivatives bearing branched citronellyl chains are designated as HAxC10Br-*M*. For simplicity, the term “alkylated” is used instead of “alkylamino hydrazide” to refer to the modified HA samples in the sequel.

Film Characterization by Confocal Microscopy, Atomic Force Microscopy, and Quartz Crystal Microbalance. Quartz crystal microbalance with dissipation monitoring (QCM-D) experiments were performed following the experimental protocol that has been extensively described in our previous publications.^{18,23} (PLL/alkylated HA)₁₈-PLL ^{FITC} films were prepared on glass slides according to the procedure described below using an automatic dipping machine^{18,23} and were imaged by confocal laser scanning microscopy (CLSM), as previously described.^{24,25} The films were also observed by atomic force microscopy (AFM) in liquid using a PicoPlus AFM with tapping mode cantilevers

(OMCL-AC240TM-E, Olympus, Germany). The rough mean square (rms) of the films was determined. The (PLL ^{FITC}/alkylated HA)₁₈ films deposited on glass slides were also viewed by fluorescence microscopy (Axiovert 200M, Zeiss, Germany) using a 10× objective. Images were obtained using a CoolSNAP EZ CCD camera and acquired with Metavue software (both from Roper Scientific, Evry, France).

Film Characterization by Fluorescence and Absorbance Measurements. For the measurement of NR incorporation by precomplexation, (PLL/alkylated HA-NR)₁₈ films were directly fabricated into 96-well plates (three wells per type of alkylated HA). Alkylated HA derivatives were precomplexed with NR by adding few μ L of a NR stock solution (1 mg/mL or 3.1 mM in ethanol) in the HA solutions at 2 g/L to have a final NR concentration of 10 μ M. Briefly, 50 μ L of PLL (1 g/L in PBS) were introduced into each well and let adsorbed for 8 min. Wells were then washed twice with the rinsing solution, and 50 μ L of alkylated HA (2 g/L in PBS) were introduced in each well, let adsorbed for 8 min, and subsequently rinsed. The process was repeated until 18 layer pairs have been deposited. The fluorescence of the plates was directly measured after each HA-NR deposition step (after the rinsing step) using a fluorescence microplate reader (Infinite 1000, Tecan, Austria) with excitation and emission wavelengths set at 590 \pm 5 nm and 650 \pm 5 nm, respectively. The absorbance at 590 \pm 2.5 nm was simultaneously measured on the same plates. For release measurements, the film fluorescence was measured at regular time intervals after removal of the supernatant and replacement by a fresh PBS solution. For estimating the absolute NR concentration, we realized a calibration curve for the absorbance of NR in the alkylated HA solutions as a function of the NR concentration, which gives a slope of 1.2×10^{-3} a.u./ μ M.

Results and Discussion

1. Synthesis of the Alkylated HA Derivatives. Because hydrophobicity of the HA derivatives is the key parameter controlling the formation of hydrophobic domains in aqueous solution, we prepared HA derivatives with alkyl chains having from 6–10 carbon atoms and degrees of substitution ranging from 0.05 to 0.1, using the methodology reported previously.¹⁴ The syntheses were performed starting from two HA samples, HA-600 and HA-200, having a weight-average molar mass of 600000 and 200000 g/mol, respectively. The alkylation procedure was based on the selective functionalization of HA by reactive dihydrazide groups^{26,27} followed by the coupling with

Table 2. Influence of the Amount of ADH Used for the Synthesis of HA-ADH **3** from HA-600 on the Intrinsic Viscosity and Huggins Coefficient Measured from Solutions in 0.01 M PBS (0.154 M NaCl, pH 7.4) at 25 °C

compound	ADH/HA ^a	K	[η] mL/g
1		0.36	1085
3	0.1	0.49	642
3	1	0.64	1099
3	2	0.74	970
3	5	0.64	953
3	10	0.77	799

^a Number of molar equiv of ADH with respect to the repeating disaccharide unit.

an aldehydic alkyl chain using reductive amination conditions (Figure 1). Although this synthetic strategy requires two steps compared to other alkylation methods of HA,^{28,29} it has the advantage of producing selectively modified polymers under mild and homogeneous conditions, thus allowing a random substitution without degradation of the HA chains. As described previously,¹⁴ the first synthetic step consisted of the reaction of HA with a large excess of difunctional adipic acid dihydrazide (10 mol equiv of ADH with respect to HA), to avoid cross-linking and rearrangement to *N*-acylurea side reactions,³⁰ in the presence of EDC (0.15 mol equiv with respect to HA) as a coupling agent. The DS of the HA-ADH conjugate was controlled by the amount of EDC used and, under such conditions, it was found to be 0.08 from ¹H NMR analysis.

In this work, we optimized the conditions for the synthesis of HA-ADH derivatives by decreasing the amount of adipic dihydrazide (ADH) used. Several assays were thus performed, in which HA-600 was reacted with variable amounts of ADH (from 10 to 0.1 mol equiv with respect to HA) in the presence of EDC (0.19 mol equiv to target a DS of 0.10). After purification of the derivatives by ultrafiltration and freeze-drying, ¹H NMR analysis confirmed the absence of any byproduct in the samples. All derivatives have a DS of 0.10 ± 0.01. The intrinsic viscosity, [η], of the products was additionally measured by capillary viscometry to get information about possible chemical cross-linking, because the value of [η] reflects the hydrodynamic volume of the polymer chain in aqueous solution. As can be seen from Table 2, the coupling of HA with ADH using amounts from 10 to 1 mol equiv did not significantly change the behavior of the polymer in aqueous solution. On the other hand, the use of 0.1 mol equiv of ADH leads to a HA-ADH derivative having an intrinsic viscosity, which is approximately two times lower than that of initial HA-600, suggesting an aggregation phenomenon or the presence of chemical cross-linking. These results show the possibility to reduce the amount of ADH used from 10 to 1 mol equiv. It can be noted that the viscosity measurements also confirmed the absence of polymer chain degradation. Indeed, as the intrinsic viscosity is related to the molar mass (*M*) of the polymer according to the Mark–Houwink equation, that is, [η] = *K*·*M*^{*a*} (where the values of the *K* and *a* constants depend on the nature of the polymer and solvent as well as on temperature), one can assume that the molar masses are similar to the initial HA and the HA-ADH derivative.

In the next step, we prepared four HA-ADH samples differing either by the initial HA substrate used (HA-600 or HA-200) or their DS (0.05 or 0.10). From the results described above, HA was reacted with 1 mol equiv of ADH in the presence of EDC (0.095 or 0.19 mol equiv with respect to HA). The resulting HA-ADH derivatives **3** were then alkylated by a reductive amination type reaction. The aldehydic hydrophobic chains

4a–d were thus coupled with HA-ADH in a water/ethanol mixture at pH 5.1, in the presence of picoline borane complex³¹ as a reducing agent, which is less toxic than previously used NaCNBH₃. The alkylated derivatives, prepared from HA-600 and HA-200, were recovered with yields in the range of 80–90% (with respect to HA-ADH) by precipitation in a mixture of aqueous 1 M NaCl and EtOH, followed by washing steps using water/EtOH mixtures. The DS of the samples was determined by ¹H NMR spectroscopy (see Figure SI-1) and are given in Table 1. It can be noted that only linear or branched chains having from 6 to 10 carbon atoms were introduced on HA as derivatives with longer chains became partially insoluble in water. The citronellal chain **4d** was selected to compare the effect of straight and branched C10 chains on the association behavior of HA in aqueous solutions and into multilayer films.

2. Associative Properties and Degradation of the HA Derivatives in Aqueous Solution. The associative properties of the alkylated derivatives were next investigated by rheological experiments from solutions in 0.01 M PBS (at pH 7.4 containing 0.154 M NaCl) at a concentration of 10 g/L, corresponding to the semidilute entangled regime of the parent HA-200 and HA-600.^{14,32} The formation of transparent gels could be macroscopically observed only for derivatives possessing linear C10 alkyl chain and, with DS higher than 0.05 in the case of HA-200. It can be noted that these results are in contrast with those reported for HA derivatives directly modified by alkyl chains through ester³³ or amide bonds.³⁴ Indeed, the formation of physical hydrogels for such derivatives required the grafting of longer alkyl chains (C16 or C18). This may be attributed to the presence of the adipic spacer arm in our case and the different experimental conditions used for the grafting of alkyl chains. Nevertheless, it can be noticed that all these derivatives have the common feature to be modified with low degrees of substitution (DS ≤ 0.1). Indeed, functionalization of HA with hydrophobic molecules at high degrees of substitution promotes the formation of poorly soluble species, which adopt a compact conformation in aqueous solution as described in the case of HA modified with the steroidal anti-inflammatory drug 6α-methylprednisolone.³⁵ Thus, the aqueous solutions of these highly modified HA derivatives exhibited viscoelastic properties more similar to HA than our HA derivatives bearing alkyl chains with low DS. The HA5C10-200 sample and the other HA-200 and HA-600 derivatives of which the lengths of grafted alkyl chains range from 6 to 8 carbon atoms lead to more or less viscous solutions. The latter were thus analyzed by steady shear viscosity measurements (Figure 2), whereas the transparent hydrogels were characterized by oscillatory shear experiments (Figure 3). As can be seen from Figure 2, most of the solutions prepared from HA5C10-200 and the HA-200 and HA-600 derivatives possessing C6, C8, and C10Br chains remain Newtonian over the range of shear rates investigated. Only the HA10C10Br-600 solution exhibits a shear-thinning behavior. This can be attributed to the disruption at high shear rates of interchain interactions due to the formation of hydrophobic domains of C10Br chains. Moreover, it can be noticed that the viscosity dependence on shear rate for the solution of HA5C6-600, HA10C6-600, HA10C8-600, and HA5C10Br-600 derivatives is lower than that of the parent polymer solution. In contrast, the viscosity dependence on shear rate for the solutions of the C6, C8, and C10Br derivatives of HA-200 is in the same range than that of the initial HA solution. Although the C6, C8, and C10Br chains are too short to form hydrophobic domains allowing the formation of a three-dimensional network, it can be reasonably assumed that alkyl chains tend to associate

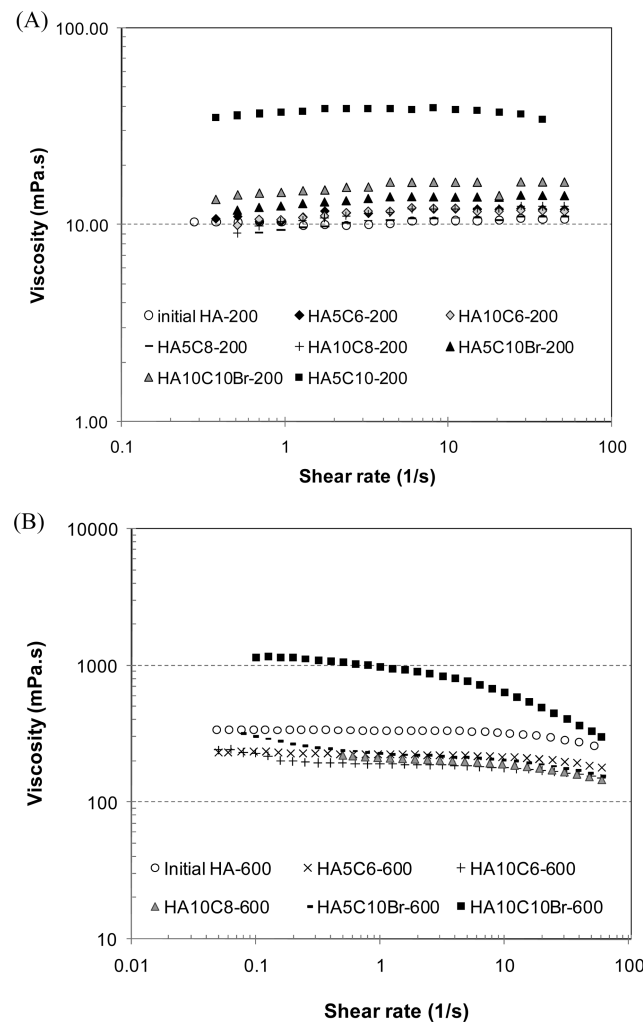


Figure 2. Viscosity dependence on shear rate of solutions of initial HA and derivatives bearing C6, C8, C10, or C10Br chains at a concentration of 10 g/L in 0.01 M PBS (0.154 M NaCl, pH 7.4). (A) samples derived from HA-200; (B) samples derived from HA-600. Due to the peculiar behavior of HA5C8 in aqueous solution, its viscosity curve is not represented.

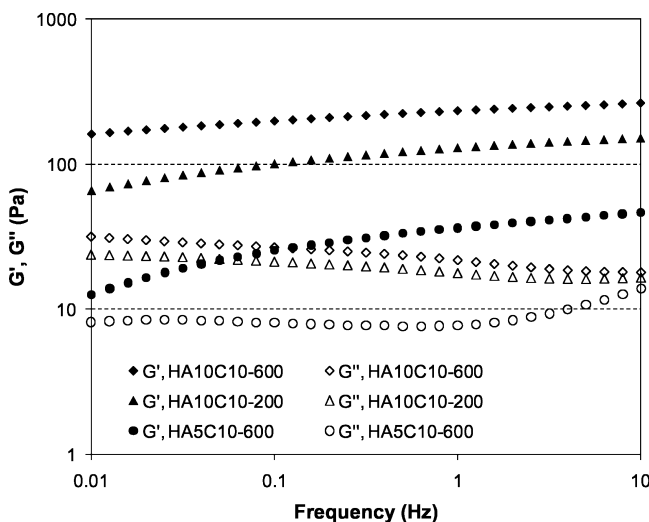


Figure 3. Comparison of the storage and loss moduli as a function of frequency for solutions of HAC10-200 and HAC10-600 derivatives (10 g/L in 0.01 M PBS (0.154 M NaCl, pH 7.4) at 25 °C).

to minimize interaction with water. In the case of HA-600, the lower values of viscosity obtained for the alkylated derivatives

compared to initial HA-600 suggest the formation of compact aggregates promoted by the hydrophobicity and the high molar mass of HA modified chains.

The dynamic rheological analysis of the HA5C10-600, HA10C10-600, and HA10C10-200 derivatives demonstrated that all the solutions behave like a highly elastic physical gel. Indeed, as can be observed in Figure 3, the storage modulus, G' , is higher than the loss modulus, G'' , over the entire range of frequencies covered. The values of the G' and G'' moduli appear to increase when the molar mass and the degree of substitution of the HA derivatives are increased.

Because the formation of a three-dimensional network is dependent on polymer concentration, we investigated the variation of the G' and G'' moduli of solutions of HA10C10-200 and HA10C10-600 derivatives as a function of the polymer concentration ($3 < C_p < 10$ g/L). In the case of HA10C10-200, a gel-like behavior ($G' > G''$ over the entire range of frequencies investigated) could be observed from concentrations equal to or higher than 5 g/L, corresponding to approximately two times the overlap concentration C^* (Supporting Information, Figure SI-2A). Below this critical concentration (C_c), HA10C10-200 gave viscoelastic or viscous solutions. In the case of HA10C10-600, this critical concentration could not be determined. Indeed, whereas macroscopic gels formed for concentrations ranging from 3.75 to 10 g/L (see Figure SI-2B), heterogeneous samples with small pieces of gels dispersed in a dilute polymer solution were obtained for concentrations lower than 3.75 g/L. For these samples, no reproducible rheological measurement was possible. Such behavior may be attributed to microgel formation, promoted by the high molar mass of HA. These results thus seem to support our previous assumption that the alkylated HA-600 derivatives show a higher tendency than their HA-200 counterparts to self-aggregate due to their higher molar mass. Differences in the association behavior depending on the polymer chain lengths were also observed for other hydrophobically modified HA derivatives.^{35,36} This was related to competitive forces existing between intramolecular interactions and internal stress according to intrinsic flexibility of the polymer backbone.³⁵ It was thus suggested that lower masses impair intramolecular interactions because of the decrease of both the number of hydrophobic groups per macromolecule and of intrinsic flexibility.³⁵

Because the hydrogels formed by HAC10-200 and -600 derivatives can be potentially degraded by tissue enzymes, such as hyaluronidases, enzymatic hydrolysis studies were performed. When the solutions of HA10C10-200 and HA5C10-600 in PBS ($C_p = 10$ g/L) were incubated at 37 °C in the presence of increasing concentrations of testicular hyaluronidase, their viscosity decreased during about 1 h. Example of result obtained for HA10C10-200 is presented in Supporting Information (Figure SI-3). A linear correlation was found between the Hase concentration and the decrease of viscosity after 4000 s, (η_{Hase}/η_{PBS} ; Figure 4). The Hase concentrations required for a 50% decrease in the viscosity of the HA derivatives in PBS (referred to as $[Hase]_{50}$) were in the range of 2 to 20 U/mL (Figure 4). The higher decrease of viscosity observed for HA-600 with respect to HA-200 for the same Hase concentration can be related to the fact that the enzymatic cleavage has a larger impact on high M_w HA samples. As reported in the literature,³⁷ the huge hydrodynamic volume of HA and simple transient intermolecular interactions, becoming more common as the molecular domains overlap, determine the viscosity. This implies that the viscosity of HA solutions may dramatically decrease when chain overlapping and intermolecular interactions are

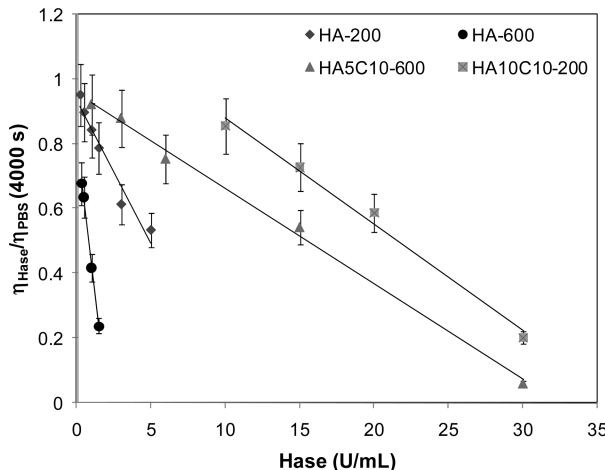


Figure 4. Variation of the $\eta_{\text{Hase}}/\eta_{\text{PBS}}$ ratio after 4000 s as a function of hyaluronidase concentration.

reduced. This may explain the high impact of chain hydrolysis observed for high M_w HA which exhibits a much higher viscous solution than HA-200 at 10 g/L in PBS (see Figure 2). Concerning the HA10C10-200 and HA5C10-600 solutions, the decrease in viscosity appears to be related to their viscoelastic properties for both modified HA samples, $[\text{Hase}]_{50}$ were about 7–8 times higher than those required for the unmodified HA ($[\text{Hase}]_{50} \sim 15 \text{ U/mL}$ for HA5C10-600 against $[\text{Hase}]_{50} \sim 2 \text{ U/mL}$ for initial HA-600). It can be noted that, in the case of the gel based on HA10C10-600, the degradation by Hase leads to heterogeneous samples with small pieces of gels dispersed in a dilute polymer solution. Therefore, reliable rheological measurements could only be performed when weakly viscous solutions ($\eta_{4000\text{s}} = 9$ and $0.75 \text{ Pa}\cdot\text{s}$) were obtained, after treatment by Hase at very high concentrations (200 and 400 U/mL, respectively). Of note, the Hase concentration in the human serum is of the order of 2.6 U/mL.³⁸ The greater resistance of the HAC10 solutions to the enzymatic hydrolysis could be due to the formation of a compact network with a lower permeability to enzymes, as suggested for chemically cross-linked HA hydrogels.^{38–40} This result is very important because it indicates that alkylation may be a useful approach to reduce the rapid degradation of HA *in vivo*, thus allowing to prolong its function. Indeed, one-third of HA is turned over each day by lymphatics and the liver in the human body.⁴¹ However, it should be noted that the physiological concentrations of Hase depends on the condition and location in the body³⁸ and that other factors such as thermal degradation and attack by free radicals are also responsible for the low residence time of endogenous HA.⁴¹

3. Formation of Multilayer Films Based on Alkylated Derivatives of HA-200 and their Ability To Entrap a Hydrophobic Dye. To investigate the potentiality of the HA-alkylated derivatives to assemble into thin multilayered films, we observed the structures of the PLL/alkylated HA multilayers using HA derivatives possessing C6, C8, C10, and C10Br chains with a DS of 0.05 and 0.10. Based on our study of the solution behavior of the alkylated HA derivatives suggesting their tendency to self-aggregate depending on the length of the alkyl chain, we selected the derivatives of HA-200 in this work.

The step-by-step film growth followed by microfluorimetry using PLL^{FITC} as labeled polyelectrolyte confirmed the regular film buildup (data not shown). AFM images of the surface of the films containing 18 layer pairs (Figure 5) and CLSM images were acquired (Figure 6). Two typical morphologies were

observed. For films made of the alkylated derivatives with C6 and C8, the film surface appears smooth similarly to the PLL/HA films (data not shown) with a rms roughness of about 1.1 nm. In contrast, for the films based on C10 and C10Br derivatives, a certain roughness was observed, which was particularly visible for the 5C10 and 10C10 containing films. Film roughnesses determined by AFM were respectively of 4.1 nm for HA5C10Br, 15.0 nm for HA10C10Br, 26.8 for HA5C10, and 98.2 nm for the HA10C10 derivative. Of note, the C10Br films appear homogeneous when observed by CLSM due to the poorer lateral resolution of this technique as compared to AFM (Figure 6A,A' and B,B'). On the other hand, “small grains” or microaggregates are visible at the surface of the films made from the HA5C10 and HA10C10 derivatives (Figure 6C,C' and D,D').

In all cases, the films were well formed on the glass substrates with similar thicknesses of about $1.8 \mu\text{m}$ for 18 layer pairs. In addition, z -section observations of the films indicate that PLL^{FITC} is able to diffuse within the films containing the alkylated derivatives similarly to that was observed previously for (PLL/HA) films.²⁴ This presence of small aggregates whose size seems to depend on the alkyl chain length and the grafting degree shares common features with previous observations performed on LbL films made of poly(acrylic acid) and hydrophobically modified poly(ethylene oxide) (HM-PEO),¹⁵ although observed at a much lower length scale. In this latter case, the very large microaggregates of $\sim 20\text{--}50 \mu\text{m}$ in size had to be imaged by profilometry and optical microscopy as they were too large to be imaged by AFM. These microaggregates were attributed to the networking or the aggregation of the HM-PEO micelles.

Slight differences in the film growth were observed for the films containing HA5C10–200 and HA10C10–200 derivatives by *in situ* measurements using quartz crystal microbalance with dissipation monitoring (QCM-D; Figure SI-4). The differences in frequency shifts as well as the viscous dissipation of the films are shown for these derivatives and compared to the unmodified HA. A high viscous dissipation was observed for the alkylated derivatives (more than 10-fold higher) as well as slightly increased frequency shifts. After the deposition of five layer pairs, the raw signals could not be fitted by the software, hence, the dissipation values and the frequency shifts could not be measured. This may be attributed to the high viscoelasticity of these films as well as to their irregular internal structure (presence of hydrophobic nanodomains coexisting with hydrophilic domains).

To investigate the potentiality of these films to trap hydrophobic dyes, we then focused on the ability of the films (built in PBS) to incorporate a hydrophobic dye, nile red. The choice of this dye was motivated by its unique properties, as its fluorescence is quenched in an aqueous environment and is intense in organic solvents or lipidic vesicles.^{42,43} NR is thus a good indicator for the presence of hydrophobic nanodomains in various types of molecules and complexes (proteins, surfactant/protein complexes)^{44,45} as well as in amphiphilic polymers.⁴⁶ Indeed, in a recent work by Glinel and co-workers,¹⁷ the UV absorbance of polyelectrolyte multilayer films containing carboxymethylpullular (CMP) grafted with C10 alkyl chains and loaded with NR was measured. In the present study, the use of a fluorescence and absorbance plate reader to measure simultaneously the red fluorescence and absorbance in films built directly in 96-well plates allows us to follow *in situ*, in an aqueous environment (PBS), the incorporation of NR. The specific properties of NR (fluorescence only in a hydrophobic environment) will thus give information of the internal structure

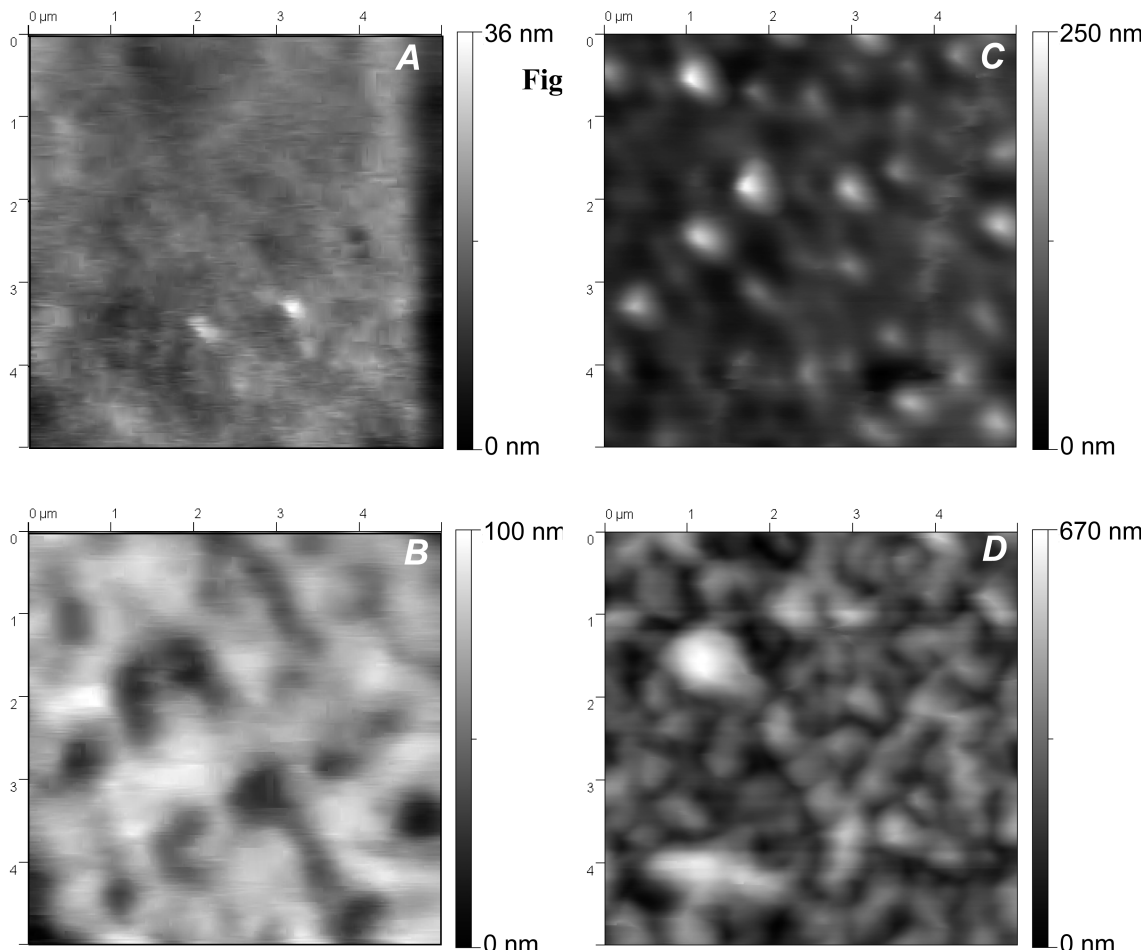


Figure 5. Topography of the films made of the HA-200 derivatives observed by AFM. All films are constituted of 18 layer pairs: (A) PLL/HA5C10Br; (B) PLL/HA10C10Br; (C) PLL/HA5C10; (D) PLL/HA10C10. Image size is $5 \times 5 \mu\text{m}^2$.

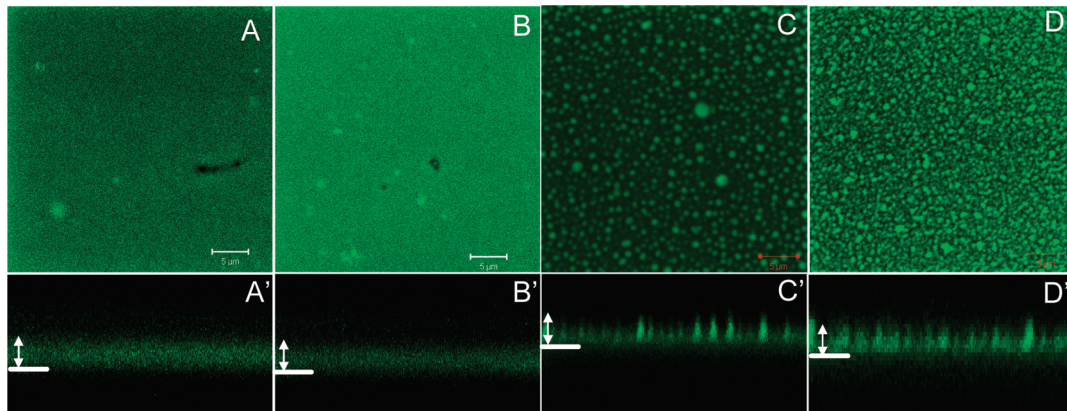


Figure 6. Typical images of different $(\text{PLL/alkylated HA-200})_{18}\text{-PLL}^{\text{FITC}}$ films observed by CLSM for (A, A') HA5C10Br, (B, B') HA10C10Br, (C, C') HA5C10, and (D, D') HA10C10 derivatives. Top views ($35.7 \times 35.7 \mu\text{m}^2$) of the films (A, B, C, D; scale bar $5 \mu\text{m}$) and zoom of the vertical sections are shown (A', B', C', D'). The borosilicate substrate (bottom of the chamber) is indicated with a white line and the white arrow (film thickness) corresponds to $\sim 1.8 \mu\text{m}$.

of the films and, in particular, on the presence of hydrophobic nanodomains.

For this study, we chose to precomplex NR with the alkylated derivatives as the dye is poorly soluble in PBS.¹⁷ We noticed at this step that the HA-NR solutions exhibit a fluorescence intensity depending on the type of alkylated derivatives (Figure 7) but no shift in excitation or emission wavelength was observed in contrary to what is commonly observed when NR is dissolved in various solvents.⁴² This qualitatively indicates that NR “sees” a similar environment. The HA10C10 derivative

exhibited the highest fluorescence, followed by the HA5C10, with all the other ones being undistinguishable.

All together, this suggests that hydrophobic nanodomains are formed in the former derivatives and that NR preferentially associates with these hydrophobic domains, whereas it remains in an aqueous environment when the alkyl chain length and DS are too small.

The step-by-step buildup of the PLL/alkylated HA-NR) films was simultaneously followed by fluorescence and absorbance measurements for the C8, C10, and C10Br chains and compared

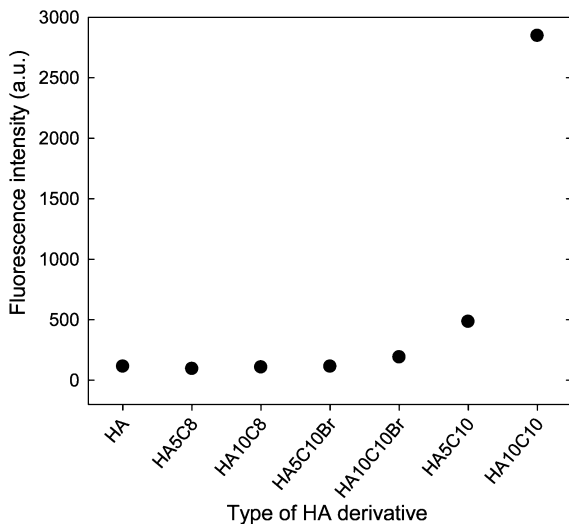


Figure 7. Fluorescence intensity of the aqueous solutions of alkylated HA-200 derivatives ($C_p = 2 \text{ g/L}$) containing nile red at a concentration of $10 \mu\text{M}$.

to that of unmodified HA (Figure 8). The fluorescence of the films containing the native HA and HA5C8 remained very low, that of HA10C8 began to grow at ~ 16 layer pairs, suggesting that these polyelectrolytes do not incorporate or incorporate very few amounts of NR. When the alkyl chain length was increased to C10Br and C10, the fluorescence significantly increased. It was indeed systematically higher for the DS of 0.1 than for 0.05. Interestingly, the simultaneous absorbance measurement of NR on the same samples indicates that NR is well present in four samples (HA5C10Br, HA10C10Br, HA5C10, and HA10C10) but that its fluorescence is significantly enhanced in the (PLL/HA10C10) films as compared to all the other ones. Linear fits of the fluorescence and absorbance curves are represented for the HA10C10 derivative (for a number of layer pairs ≥ 6) and for the HA10C10Br derivative (for a number of layer pairs ≥ 11). The slope for the fluorescence was ~ 3.5 higher for HA10C10 as compared to HA10C10Br (135.3 vs 37.4), but the slope for absorbance was very similar for both derivatives (0.0179 vs 0.0175). This indicates a more pronounced hydrophobic environment for NR solubilized in the microdomains of C10 chains. The fact that at least six layers is required before any absorption is detected suggests a minimum intensity is required: the resolution of the apparatus for NR measurement can be estimated at 0.005, which corresponds to a concentration of $3 \mu\text{M}$ in our experimental conditions (or 0.9 nanomoles). Below this concentration, it is thus not possible to detect the presence of NR. This may also partly be due to the fact that the layers are too immature to hold sufficient NR, as PLL/HA films are known to first form isolated islets before the films become continuous.⁴⁷ An estimate of the concentration of NR in the films was deduced from the calibration curve and by considering that the volume of the film in the well is $6.5 \times 10^{-4} \text{ cm}^3$ (film thickness taken as $1.8 \mu\text{m}$ and surface of the well 0.36 cm^2). The number of NR moles in the HA10C10 films is ~ 33 nanomoles, whereas it is between 18–22 nanomoles for the three other ones (HA5C10Br, HA10C10Br, and HA5C10). This corresponds to an “effective” concentration in the film of 51 mM for HA10C10 and of 28–34 mM for the other ones, which represents an ~ 5000 -fold increase in NR concentration upon loading in the films as compared to its initial concentration in solution. Such films have thus a very high capacity of retaining the dye at a very high local concentration.

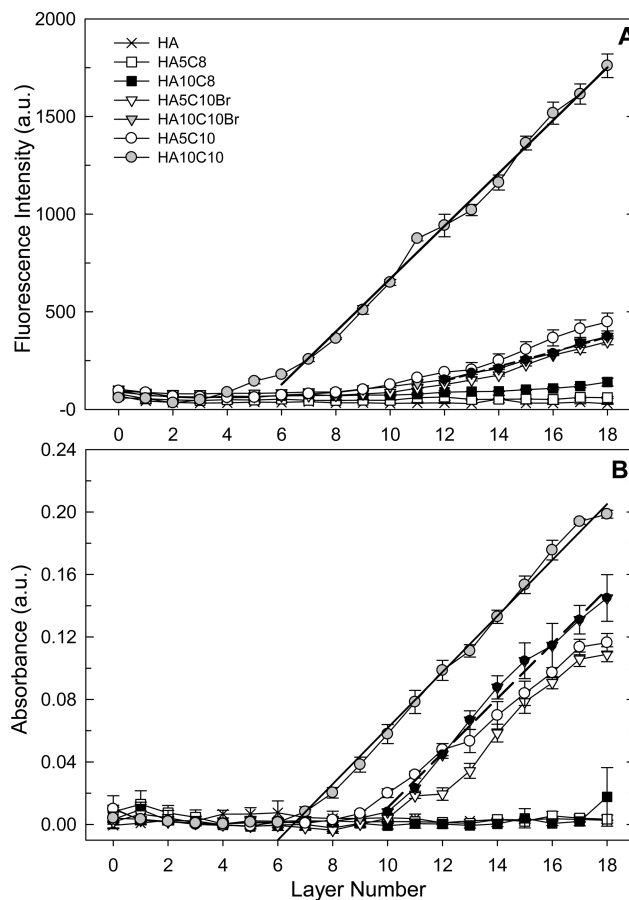


Figure 8. (A) Nile red incorporation in the (PLL/alkylated HA-200 derivatives)₁₈ films followed by a fluorescence microplate reader after each deposition step of the polyanion; (B) Absorbance measurements at $590 \pm 2.5 \text{ nm}$ performed on the same films. Linear fits for the HA10C10 (plain lines) and HA10C10Br derivatives (dotted lines) are shown in (A) and (B). For the fluorescence curves, the slopes are, respectively, 135.3 (calculated for $i \geq 6$) and 37.4 (calculated for $i \geq 10$) for these derivatives; for the absorbance curves, the slopes calculated over the same range are similar, with respective values of 0.0179 and 0.0175.

All together, these results show the strong ability of the HA10C10 and HA5C10 (and in a lesser extent HA10C10Br and HA5C10Br) to trap the dye into hydrophobic nanodomains. Noticeably, the dye remained trapped in the hydrophobic nanodomains once the complex is absorbed on the surface and thus, a continuous increase in fluorescence is observed when the number of deposited layer pairs increases.

Interestingly, not only the HA10C10 that behaves like a physical gel in solution at high concentrations (10 g/L) could incorporate NR but also the other derivatives in C10 and C10Br. Importantly, the layering of the HA alkylated derivatives in thin films as well as the presence of PLL do not hinder the formation of these domains. These results also suggest that the hydrophobic domains would still be present in films assembled without dye.

Of note, we also attempted to build the HA10C10 films in a mixture of water/DMSO to investigate how the solvent could affect the film buildup properties and its loading properties. We observed an effect on the surface morphology, the films exhibited a lower roughness when the % of DMSO is increased (Figure SI-5). However, this also led to a drastic reduction of hydrophobic dye incorporation, suggesting that the number of hydrophobic nanodomains is greatly reduced in these conditions, presumably due to a disruption of the hydrophobic interactions (increased solubilization) when the modified HA is surrounded

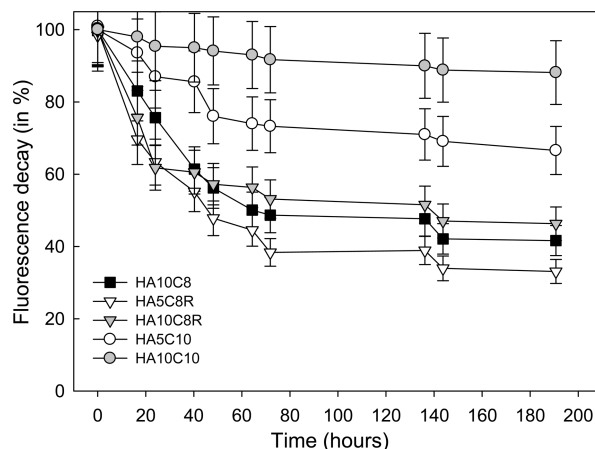


Figure 9. Nile red release from the different films in PBS at 37 °C as a function of the time. For clarity, the HA and HA5C8 that exhibited a very small fluorescence intensity and a nondetectable absorbance (see Figure 8 above) were not represented.

by DMSO. This further shows that the hydrophobic nanodomains have to be present for the hydrophobic dye to be loaded in the films and that the formation of these domains influences the film microstructure (increased roughness for more hydrophobic films).

To further investigate the properties of these films, their stability in PBS at 37 °C of the NR containing films was investigated over an 8 day period (Figure 9). The HA10C8, HA5C10Br, and HA10C10Br exhibited the highest decay in fluorescence of ~40–60% over the whole period, with a plateau value being reached in about 3 days. Interestingly, the fluorescence decay for films built with the HA5C10 and HA10C10 derivatives was only ~20 and ~10%, respectively, which further suggests that the dye is more strongly interacting with the HA chains and thus more stabilized in these films.

Conclusions

Several amphiphilic derivatives of HA were synthesized by varying the length of the grafted alkyl chains, the degree and substitution, and the molecular weight of the HA backbone to design new platforms for delivery of hydrophobic drugs. Remarkable self-associating properties were observed for derivatives having C10 chains, giving rise to three-dimensional physical hydrogels in semidilute aqueous solution. This was related to the formation of hydrophobic nanodomains playing the role of junction points, as demonstrated by fluorescence probing. Interestingly, the formation of hydrophobic nanodomains could also be observed when alkylated HA derivatives were self-assembled into planar multilayer thin films by polyelectrolyte complexation with PLL. Their ability to entrap hydrophobic molecules was found to be tunable according to the HA derivative selected for the construction of the film and its thickness, which was related to the number of deposited layers. Similar to results obtained in the bulk, the HA10C10 derivative lead to films able to efficiently entrap the dye nile red into hydrophobic nanodomains. This was demonstrated not only by the strong increase of fluorescence intensity of NR during the film buildup, but also by the lower fluorescence decay observed for these films upon storage. Considering the promising properties of these films as drug delivery systems, we plan in future work to investigate the incorporation and biological activity of anticancer agents loaded in such films.

Acknowledgment. This work has been supported by “Agence Nationale pour la Recherche” (Grant ANR-06-NANO-006 to

C.P. and ANR-07-NANO-002 to R.A.-V. and C.P.). We thank Judith Mähner for her technical help in experiments using the microplate reader. C.P. is a Junior Member of the “Institut Universitaire de France” whose support is gratefully acknowledged. S.K. and D.C. gratefully acknowledge ARD and the MENRT, respectively, for their thesis grant in CERMAV.

Supporting Information Available. ¹H NMR spectrum of HA10C10-200; storage and loss moduli dependence on frequency for HA10C10-200 and HA10C10-600 at various concentrations in PBS; kinetics of HA10C10-200 degradation by viscosity measurement in the presence of different concentrations of testicular hyaluronidase in PBS and its discussion; and QCM-D profiles obtained for (PLL/HA5C10) and (PLL/HA10C10) film growth in PBS; fluorescence microscopy observations of (PLL/HA10C10)₁₈ films built up in mixtures of water and DMSO at increasing percentages. This material is available free of charge via the Internet at <http://pubs.acs.org>.

References and Notes

- Allison David, D.; Grande-Allen, K. J. *Tissue Eng.* **2006**, *12*, 2131–2140.
- Kogan, G.; Soltes, L.; Stern, R.; Gemeiner, P. *Biotechnol. Lett.* **2007**, *29*, 17–25.
- Morra, M. *Biomacromolecules* **2005**, *6*, 1205–1223.
- Prestwich, G. D.; Kuo, J.-w. *Curr. Pharm. Biotechnol.* **2008**, *9*, 242–245.
- Prestwich, G. D.; Shu, X. Z.; Liu, Y.; Cai, S.; Walsh, J. F.; Hughes, C. W.; Ahmad, S.; Kirker, K. R.; Yu, B.; Orlandi, R. R.; Park, A. H.; Thibeault, S. L.; Duflo, S.; Smith, M. E. *Adv. Exp. Med. Biol.* **2006**, *585*, 125–133.
- Shu, X. Z.; Prestwich, G. D. In *Chemistry and Biology of Hyaluronan*; Garg, H. G., Hales, C. A., Eds; Elsevier Ltd.: New York, 2004, 475–504.
- Vercruyse, K. P.; Prestwich, G. D. *Crit. Rev. Ther. Drug Carrier Syst.* **1998**, *15*, 513–555.
- Yadav, A. K.; Mishra, P.; Agrawal, G. P. *J. Drug Targeting* **2008**, *16*, 91–107.
- Fraser, J. R. E.; Laurent, T. C.; Laurent, U. B. G. *J. Intern. Med.* **1997**, *242*, 27–33.
- Abatangelo, G.; Weigel, P. H.; Eds. In *New Frontiers in Medical Sciences: Redefining Hyaluronan*; Elsevier Science B.V.: New York, 2000; p 372.
- Chen, W. Y.; Abatangelo, G. *Wound Repair Regen.* **1999**, *7*, 79–89.
- Entwistle, J.; Hall, C. L.; Turley, E. A. *J. Cell. Biochem.* **1996**, *61*, 569–577.
- Toole, B. P. *J. Intern. Med.* **1997**, *242*, 35–40.
- Creuzet, C.; Kadi, S.; Rinaudo, M.; Auzély-Velty, R. *Polymer* **2006**, *47*, 2706–2713.
- Seo, J.; Lutkenhaus, J. L.; Kim, J.; Hammond, P. T.; Char, K. *Macromolecules* **2007**, *40*, 4028–4036.
- Seo, J.; Lutkenhaus, J. L.; Kim, J.; Hammond, P. T.; Char, K. *Langmuir* **2008**, *24*, 7995–8000.
- Guyomard, A.; Nysten, B.; Muller, G.; Glinel, K. *Langmuir* **2006**, *22*, 2281–2287.
- Schneider, A.; Vodouhe, C.; Richert, L.; Francius, G.; Le Guen, E.; Schaaf, P.; Voegel, J.-C.; Frisch, B.; Picart, C. *Biomacromolecules* **2007**, *8*, 139–145.
- Vodouhe, C.; Le Guen, E.; Garza, J. M.; Francius, G.; Dejugnat, C.; Ogier, J.; Schaaf, P.; Voegel, J.-C.; Lavalle, P. *Biomaterials* **2006**, *27*, 4149–4156.
- Thierry, B.; Kujawa, P.; Tkaczyk, C.; Winnik, F. M.; Bilodeau, L.; Tabrizian, M. *J. Am. Chem. Soc.* **2005**, *127*, 1626–1627.
- Auzély-Velty, R.; Rinaudo, M. *Macromolecules* **2002**, *35*, 7955–7962.
- Huggins, M. L. *J. Am. Chem. Soc.* **1942**, *64*, 2716–2718.
- Richert, L.; Lavalle, P.; Payan, E.; Shu Xiao, Z.; Prestwich Glenn, D.; Stoltz, J.-F.; Schaaf, P.; Voegel, J.-C.; Picart, C. L. *Langmuir* **2004**, *20*, 448–458.
- Picart, C.; Mutterer, J.; Richert, L.; Luo, Y.; Prestwich, G. D.; Schaaf, P.; Voegel, J. C.; Lavalle, P. *Proc. Natl. Acad. Sci. U.S.A.* **2002**, *99*, 12531–12535.
- Richert, L.; Schneider, A.; Vautier, D.; Vodouhe, C.; Jessel, N.; Payan, E.; Schaaf, P.; Voegel, J.-C.; Picart, C. *Cell Biochem. Biophys.* **2006**, *44*, 273–285.

- (26) Kirker, K. R.; Prestwich, G. D. *J. Polym. Sci., Part B* **2004**, *42*, 4344–4356.
- (27) Prestwich, G. D.; Marecak, D. M.; Marecek, J. F.; Vercruyse, K. P.; Ziebell, M. R. *J. Controlled Release* **1998**, *53*, 93–103.
- (28) Mlcochova, P.; Bystricky, S.; Steiner, B.; Machova, E.; Koos, M.; Velebny, V.; Krcmar, M. *Biopolymers* **2006**, *82*, 74–79.
- (29) Mlcochova, P.; Hajkova, V.; Steiner, B.; Bystricky, S.; Koos, M.; Medova, M.; Velebny, V. *Carbohydr. Polym.* **2007**, *69*, 344–352.
- (30) Pouyani, T.; Kuo, J. W. *J. Am. Chem. Soc.* **1992**, *114*, 5972–5976.
- (31) Sato, S.; Sakamoto, T.; Miyazawa, E.; Kikugawa, Y. *Tetrahedron* **2004**, *60*, 7899–7906.
- (32) Charlot, A.; Auzély-Velty, R. *Macromolecules* **2007**, *40*, 9555–9563.
- (33) Pelletier, S.; Hubert, P.; Payan, E.; Marchal, P.; Choplin, L.; Dellacherie, E. *J. Biomed. Mater. Res.* **2001**, *54*, 102–108.
- (34) Finelli, I.; Chiessi, E.; Galessio, D.; Renier, D.; Paradossi, G. *Macromol. Biosci.* **2009**, *9*, 646–653.
- (35) Taglienti, A.; Valentini, M.; Sequi, P.; Crescenzi, V. *Biomacromolecules* **2005**, *6*, 1648–1653.
- (36) Mravec, F.; Pekar, M.; Velebny, V. *Colloid Polym. Sci.* **2008**, *286*, 1681–1685.
- (37) Cowman, M. K.; Matsuoka, S. *Carbohydr. Res.* **2005**, *340*, 791–809.
- (38) Leach, J. B.; Bivens, K. A.; Patrick, C. W., Jr.; Schmidt, C. E. *Biotechnol. Bioeng.* **2003**, *82*, 578–589.
- (39) Burdick Jason, A.; Chung, C.; Jia, X.; Randolph Mark, A.; Langer, R. *Biomacromolecules* **2005**, *6*, 386–391.
- (40) Lee, F.; Chung, J. E.; Kurisawa, M. *Soft Matter* **2008**, *4*, 880–887.
- (41) Sall, I.; Ferard, G. *Polym. Degrad. Stab.* **2007**, *92*, 915–919.
- (42) Greenspan, P.; Fowler, S. D. *J. Lipid Res.* **1985**, *26*, 781–789.
- (43) Greenspan, P.; Mayer, E. P.; Fowler, S. D. *J. Cell Biol.* **1985**, *100*, 965–973.
- (44) Daban, J. R.; Samso, M.; Bartolome, S. *Anal. Biochem.* **1991**, *199*, 162–168.
- (45) Sackett, D. L.; Wolff, J. *Anal. Biochem.* **1987**, *167*, 228–234.
- (46) Gautier, S.; Bousta, M.; Vert, M. *J. Controlled Release* **1999**, *60*, 235–247.
- (47) Picart, C.; Lavalle, P.; Hubert, P.; Cuisinier, F. J. G.; Decher, G.; Schaaf, P.; Voegel, J. C. *Langmuir* **2001**, *17*, 7414–7424.

BM900701M